CILAMCE 2017
Florianópolis - Santa Catarina - Brazil

AN ALTERNATIVE APPROACH TO THE ISOTROPIC ERROR DENSITY RECOVERY METHOD BASED ON LOCAL PATCHES

Frederico Alves Jahnert[1]

Jucélio Tomás Pereira[1]

Jéderson da Silva[1,2]

fred_jahnert@hotmail.com

dasilva.jerderson@gmail.com

jucelio.tomas@ufpr.br

[1]Programa de Pós-Graduação em Engenharia Mecânica – Universidade Federal do Paraná

Rua Cel. Francisco H. dos Santos, 210, Paraná, Curitiba, Brasil.

[2]Universidade Tecnológica Federal do Paraná

Avenida dos Pioneiros, Jardim Morumbi, 3131, Paraná, Londrina, Brasil.

Abstract. *The h-adaptive Finite Element Method based on a posteriori error estimation has demonstrated to be a valuable tool regarding the control and limitation of approximation errors contained in the solution. This study aims at obtaining an efficient mesh refinement methodology by proposing a modification to the Isotropic Error Density Recovery (IEDR) h-adaptive mesh refinement method. Originally, the IEDR technique was introduced using triangular finite elements with linear approximation, where the new element's sizes are calculated by evaluating a quadratic error density function in energy at the element's centroid. Conversely, the current article proposes defining a quadratic error density function in energy with origin at each node of the mesh. This is carried out by utilizing patches of elements formed by all the elements sharing the node to be evaluated. This new methodology, named here as Isotropic Error Density Nodal Recovery (IEDNR) offers a way to evaluate the new element parameters directly in each node of the mesh and presents itself as an approach to generalize the IEDR technique for any polynomial order of approximation. The efficiency of the IEDNR methodology is analyzed in elliptic two-dimensional problems utilizing first order finite elements.*

Keywords: *Finite Element Method, h-adaptivity, Superconvergent Patch Recovery, Isotropic Error Density Recovery.*

1 INTRODUCTION

The numerical solution obtained through the use of the finite element method is heavily dependent on the mesh configuration. The approximative nature of the method requires an efficient mesh discretization in order to obtain a suitable solution while maintaining a low computational cost. In this context, h-adaptive refinement methodologies have been put forward as a solution to this problem. Considering an h-adaptive process, two main steps are required: estimation of element error distribution – this is achieved by the use of error estimators – and definition of a new mesh design.

A great effort has been put into the development of error estimators in order to evaluate discretization errors (Reddy, 2006). These can be classified into two main categories, *a priori* error estimators and *a posteriori* error estimators. *a priori* error estimators are applied before the finite element solution is calculated, whereas the *a posteriori* error estimator is used after the finite element solution is found (Ainsworth and Oden, 2000). The latter can be divided into two distinct types of error estimators, recovery based error estimators and residual based recovery estimators.

Introduced by Zienkiewicz and Zhu (1987), recovery based error estimators have proven to be economical and effective in evaluating errors (Zienkiewicz and Zhu, 1992b). The essence of this procedure is to compare the finite element solution with a more convergent recovered solution as a measure of local error (Zienkiewicz and Taylor, 2000). In order to obtain precise error estimation, many efficient solution recovery techniques have been developed in the literature. Some noticeable examples are: the Superconvergent Patch Recovery (SPR) (Zienkiewicz and Zhu, 1992a, 1992b), the Superconvergent Patch Recovery with Equilibrium (SPRE) (Wiberg and Abdulwahab, 1992), the Superconvergent Patch Recovery incorporating Equilibrium and Boundary conditions (SPREB) (Wiberg et al., 1994), the Recovery by Equilibrium of Patches (REP) (Boroomand and Zienkiewicz, 1997), the Recovery by Compatibility in Patches (RCP) (Ubertini, 2004; Benedetti et al., 2006; Castellazzi et al., 2010), the Polynomial Preserving Recovery (PPR) (Zhang and Naga, 2005) and The Superconvergent Cluster Recovery Method (SCR) (Huang and Yi, 2010).

Adaptive processes have been applied to the finite element method as ways to ensure an optimal mesh discretization. According to Cook *et al.* (2002), three main adaptive refinement processes are known: h-adaptativity, concerning the size of the elements in the mesh, p-adaptivity, concerning the polynomial order p of each element approximation, and r-adaptivity, which is related to the location of the nodes in the mesh. Currently, the most common methodology in the literature for h-adaptive refinement using a recovery based error estimator is the Ch^p technique (Zienkiewicz and Zhu, 1987). After acquiring the local error distribution, the Ch^p technique revolves around the concept that the error is proportional to the size of the element raised to the power p, where p is the order of the element approximation. This methodology defines that the global error should be equally distributed in each element. Other mentionable mesh design methodologies are the Li-Bettess technique and the Díez-Huerta unified approach (Li and Bettess, 1995; Díez and Huerta, 1999).

Recently, Pereira *et al.* (2016) and Silva and Pereira (2017) have proposed a new h-adaptivity process called Isotropic Error Density Recovery (IEDR). It simultaneously makes use of the concept of recovery of the error density function in the energy norm and the analytical solution of an optimization problem via the Lagrange Multiplier Method to find the optimal size of the new element. Although only for linear element approximations, the IEDR has shown results that minimize error while maintaining a low number of degrees of freedom.

This article proposes a modification to this technique, called Isotropic Error Density Nodal Recovery (IEDNR), where the recovery of the error density function in the energy norm is used to average a nodal error density function. Hence, the new element parameters are evaluated directly in each node of the mesh. The IEDNR methodology is tested and compared – in the context of linear scalar elliptic problems – with the Ch^p and IEDR methodology. Mesh generation is performed using BAMG (Bidimensional Anisotropic Mesh Generator), which is part of the Freefem++ software (Hecht, 2012).

2 PROBLEM MODEL AND DISCRETIZATION ERROR ESTIMATION

To illustrate the idea behind the methodology, a generic elliptic scalar problem of the Poisson type, defined in a domain Ω, can be expressed as:

$$\begin{aligned} &\text{Find } u(x,y) \in H^1(\Omega) \\ &\int_\Omega (\nabla v)^T \boldsymbol{k} \nabla u \, d\Omega = \int_\Omega v f \; d\Omega, \quad \forall \quad v \in H_0^1(\Omega), \end{aligned} \tag{1}$$

where u is the analytical solution, $\boldsymbol{k}$ is a constant isotropic tensor, f is the scalar function of domain excitation, ∇ is the gradient differential operator, v is a function of a generic kinematically admissible variation and H_0^1 denotes first-order Hilbert space with compact support in Ω. The solution of the problem, Eq. (1), can be obtained using FEM. Considering an h-adaptive process, the error distribution originated from the element approximations are required to be evaluated. According to Zienkiewicz and Zhu (1987), the element error can be estimated in the energy norm ($\|e\|$) as:

$$\|e\| = \left[\int_\Omega \left(\nabla u - \nabla u^{FEM} \right)^T \boldsymbol{k} \left(\nabla u - \nabla u^{FEM} \right) d\Omega \right]^{1/2}, \tag{2}$$

where ∇u^{FEM} is the gradient of the FEM solution. Bearing in mind that the analytical solution (∇u) is unknown, an estimate for the element's error in the energy norm $\left(\|e^{REC}\|\right)$ is given by

$$\|e^{REC}\| = \left[\int_\Omega \left(\nabla u^{REC} - \nabla u^{FEM} \right)^T \boldsymbol{k} \left(\nabla u^{REC} - \nabla u^{FEM} \right) d\Omega \right]^{1/2}. \tag{3}$$

In this case, ∇u^{REC} denotes the gradient vector recovered from the FEM solution which is obtained using gradient recovery methods. In this paper, the SPR technique is utilized by virtue of its accurate estimations and simplicity (Zienkiewicz and Zhu, 1992a, 1992b). The error estimator quality can be measured using the effectiveness index, θ, defined as the ratio between the estimated and the real error. Thus, if the recovered solution converges with a higher rate than that of the FEM solution, one would have an asymptotically exact estimate (Zienkiewicz and Zhu, 1992b).

3 *h*-ADAPTIVITY MESH REFINEMENT STRATEGIES

The distribution of error in the energy norm can be used to determine which elements need to be refined and which one need to be increased in size. A common mesh refinement strategy is to seek to equidistribute the error equally between the elements along the mesh. It can be defined that an acceptable solution is one which the global error in energy norm $\left(\|e\|\right)$ is not greater than a specified percentage of the total energy. This can be expressed as

$$\|e\| \le \bar{\eta}\,\|u\|, \tag{4}$$

where $\bar{\eta}$ is the relative global error defined by the user and $\|u\|$ is the total potential energy of the system, given by

$$\|u\| = \left[\int_{\Omega} (\nabla u)^T \boldsymbol{k} (\nabla u)\, d\Omega\right]^{\frac{1}{2}}. \tag{5}$$

This expression is modified due to the unknowingness of the solution. Rearranging in terms of FEM's solution total potential energy and utilizing the error's orthogonality property (Oden and Reddy, 2011), the total energy of the system can be expressed as

$$\|u\| = \left(\left\|u^{FEM}\right\|^2 + \left\|e^{REC}\right\|^2\right)^{\frac{1}{2}}, \tag{6}$$

where

$$\left\|u^{FEM}\right\| = \left[\int_{\Omega} \left(\nabla u^{FEM}\right)^T \boldsymbol{k} \left(\nabla u^{FEM}\right) d\Omega\right]^{\frac{1}{2}}. \tag{7}$$

According to Zienkiewicz and Zhu (1987), the admissible error in energy in each element $\left(\varepsilon_{adm}\right)$ can then be defined as the division of the total admissible error by the number of elements (NEl), giving

$$\varepsilon_{adm} = \bar{\eta}\,\|u\| \big/ \sqrt{NEl}\,. \tag{8}$$

3.1 The Ch^p mesh design technique

Introduced by Zienkiewicz and Zhu (1987), the Ch^p technique has been widely used in many h-adaptivity problems (Wiberg et al., 1997; Díez and Huerta, 1999; Onãte and Bugeda, 1993; Castellazzi et al., 2010). This technique proposes the equidistribution of the error in energy norm by subdividing elements proportionally to the rate of convergence of the error, $O(h^p)$. The element refinement parameter, ζ_{ie}, in terms of the element error, $\|e\|_{ie}$, is given by

$$\zeta_{ie} = \frac{\|e\|_{ie}}{\varepsilon_{adm}}. \tag{9}$$

Proceedings of the XXXVIII Iberian Latin-American Congress on Computational Methods in Engineering
P.O. Faria, R.H. Lopez, L.F.F. Miguel, W.J.S. Gomes, M. Noronha (Editores), ABMEC, Florianópolis, SC, Brazil, November 5-8, 2017.

Equation (9) relates the element error to the maximum allowable element error. If $\zeta_{ie} > 1$ the element should be decreased in size, otherwise the element should be enlarged. As mentioned, the Ch^p technique utilizes the convergence rate of the error estimator at element level as basis of the h-adaptive, given by

$$\|e\| \leq Ch^{min(p,\lambda)}, \tag{10}$$

where C is a constant, h represents the size of the finite element, p is the polynomial order of approximation of the element and λ is a parameter defining the intensity of possible singularities in the element (Zienkiewicz and Taylor, 2000). Disregarding singularities, the new element size (h_{new}) is found by comparing the element error (Eq. (9) and Eq. (10)) between the current mesh and the next mesh, given by

$$h_{new} = \frac{h_{old}}{\zeta_{ie}^{1/p}}, \tag{11}$$

where h_{old} is the element size in the current mesh.

3.2 Isotropic Error Density Recovery (*IEDR*) technique

As proposed by Pereira *et al*. (2016) and Silva and Pereira (2017), the IEDR technique recovers a quadratic equation for the error density function in the energy norm with origin at the centroid of the element. Thus, the total error in any area Ω_{ie} for the *ie-th* element can be evaluated as

$$\left\|e^{REC}\right\|^2 = \int_{\Omega_{ie}} U \, d\Omega = \int_{\Omega_{ie}} \Delta\boldsymbol{u}^T \boldsymbol{k} \, \Delta\boldsymbol{u} \, d\Omega, \tag{12}$$

where U is the error density function of the error in energy, while $\Delta\boldsymbol{u}$ denominates the gradient error vector, expressed as the difference between gradients obtained through FEM and the recovered gradient:

$$\Delta\boldsymbol{u} = \nabla\boldsymbol{u}^{REC} - \nabla\boldsymbol{u}^{FEM}. \tag{13}$$

Thus, the density function of the error in energy can be written as

$$U = U(x,y) = \Delta u^T \boldsymbol{k} \, \Delta u = \boldsymbol{P}^T \boldsymbol{B}_{\nabla u}^T \boldsymbol{k} \boldsymbol{B}_{\nabla u} \boldsymbol{P} = \boldsymbol{P}^T \boldsymbol{Z} \boldsymbol{P}, \tag{14}$$

where $\boldsymbol{P}$ is a vector which contains the relative coordinates of a generic point, $\boldsymbol{B}_{\nabla u}$ is a matrix with the coefficients of the recovered gradient polynomial equation and $\boldsymbol{Z}$ represents a symmetric matrix defined by the product

$$\boldsymbol{Z} = \boldsymbol{B}_{\nabla u}^T \boldsymbol{k} \boldsymbol{B}_{\nabla u}. \tag{15}$$

The expansion of this density function of error $U(x,y)$ results in

$$
\begin{aligned}
U(x,y) &= \boldsymbol{P}^T \boldsymbol{Z}\boldsymbol{P} = \\
&= (Z_{11}) + (Z_{12}+Z_{21})x + (Z_{13}+Z_{31})y + \left[Z_{22}x^2 + (Z_{23}+Z_{32})xy + Z_{33}y^2\right] \\
&= U_0 + (G_1 x + G_2 y) + \left(H_{11}x^2 + 2H_{12}xy + H_{22}y^2\right) \\
&= U_0 + \boldsymbol{G}\boldsymbol{x} + \boldsymbol{x}^T \boldsymbol{H}\boldsymbol{x}\,,
\end{aligned}
\tag{16}
$$

where U_0, $\boldsymbol{G}$, $\boldsymbol{H}$ and $\boldsymbol{x}$ are given by

$$U_0 = Z_{11}, \tag{17}$$

$$\boldsymbol{G} = \begin{Bmatrix} G_1 \\ G_2 \end{Bmatrix} = \begin{Bmatrix} Z_{12}+Z_{21} \\ Z_{13}+Z_{31} \end{Bmatrix}, \tag{18}$$

$$\boldsymbol{H} = \begin{bmatrix} H_{11} & H_{12} \\ H_{21} & H_{22} \end{bmatrix} = \begin{bmatrix} Z_{22} & Z_{23} \\ Z_{32} & Z_{33} \end{bmatrix}, \tag{19}$$

$$\boldsymbol{x} = \begin{Bmatrix} x \\ y \end{Bmatrix}. \tag{20}$$

In this case, U_0 is the constant term of the equation, $\boldsymbol{G}$ is a vector containing the coefficients of the linear terms, $\boldsymbol{H}$ is the Hessian matrix associated with the quadratic terms of the error density function and $\boldsymbol{x}$ is a vector of relative coordinates with origin at the centroid of the element.

By evaluating an element's error density function in energy, the size of the new element is found through the integral of the function over a concentric triangular domain. Thus, the error in energy norm, E_{ie}^2, expressed for a generic triangular domain, Ω_{ie}, is given by

$$
\begin{aligned}
E_{ie}^2 &= \int_{\Omega_{ie}} U\, d\Omega = \int_{\Omega_{ie}} \left[U_0 + (G_1 x + G_2 y) + \left(H_{11}x^2 + 2H_{12}xy + H_{22}y^2\right)\right] d\Omega \\
&= U_0 \int_{\Omega_{ie}} d\Omega + G_1 \int_{\Omega_{ie}} x\, d\Omega + G_2 \int_{\Omega_{ie}} y\, d\Omega + H_{11} \int_{\Omega_{ie}} x^2\, d\Omega \ldots \\
&\quad \ldots + 2H_{12} \int_{\Omega_{ie}} xy\, d\Omega + H_{22} \int_{\Omega_{ie}} y^2 d\Omega.
\end{aligned}
\tag{21}
$$

The integral of the function over a triangular domain nullifies the second, third and fifth terms of Eq. (21) due to symmetry and the coincident coordinate system. Thus, Eq. (21) can be expressed as

$$E_{ie}^2 = U_0 A_{ie} + H_{11} I_y + H_{22} I_x, \tag{22}$$

where A_{ie} denotes the area of the triangle while I_x and I_y are the geometry's second moments of area, described by Eq. (23),

$$
\begin{aligned}
A_{ie} &= \int_{\Omega_{ie}} d\Omega = \alpha h^2, \quad com \quad \alpha = \sqrt{3}/4, \\
I_x &= \int_{\Omega_{ie}} y^2 d\Omega = I_y = \int_{\Omega_{ie}} x^2\, d\Omega = \beta h^4, \quad com \quad \beta = \sqrt{3}/96.
\end{aligned}
\tag{23}
$$

Thus, the error contained in the triangular region, with edge size h, can be defined as

$$E_{ie}^{2}=h^{2}\left[\alpha U_{0}+\beta tr(\boldsymbol{H})h^{2}\right], \tag{24}$$

where $tr(\boldsymbol{H})=H_{11}+H_{22}$.

The isotropic element design occurs by utilizing an optimization technique to maximize the size of a triangle – with edge size h_{new} and concentric with the original element with edge size h_{old} – restricted to $E_{o}^{2}\le\varepsilon_{adm}^{2}$. The optimization problem can be stated as

$$P:\begin{cases} minimize & -h \\ Constraint: & g(h)\le 0, \end{cases} \tag{25}$$

$g(h)$ can be defined as an inequality constraint, expressed as

$$g(h)=E_{o}^{2}-\varepsilon_{adm}^{2}=h^{2}\left[\alpha U_{0}+\beta tr(\mathrm{H})h^{2}\right]-\varepsilon_{adm}^{2}. \tag{26}$$

The solution of the optimization problem is evaluated utilizing Lagrange multipliers by submitting it to necessary conditions of optimality. The solution of the problem is expressed as

$$\beta tr(\boldsymbol{H})h^{4}+\alpha U_{0}h^{2}-\varepsilon_{adm}^{2}=0 \tag{27}$$

The positive root of Eq. (27) is given by

$$h_{new}=\left(\frac{\sqrt{(\alpha U_{0})^{2}+4\beta tr(\boldsymbol{H})\varepsilon_{adm}^{2}}-\alpha U_{0}}{2\beta tr(\boldsymbol{H})}\right)^{1/2}. \tag{28}$$

Accordingly, Eq. (28) is applied to every element of the mesh in order to define the new mesh parameters.

3.2.1 Admissible error update considering optimal mesh

The definition of the element admissible error in h-adaptive analysis is based on the definition of an optimal mesh criterion. Silva and Pereira (2017) introduced an iterative process that uses optimal mesh properties based on comparing the current mesh to the next mesh.

As aforementioned, Zienkiewicz and Zhu (1987), defined that an optimal mesh distributes the global error equally in each element. As an example, Li and Bettess (1995) proved that the error in energy norm should be used to equally divide the error between each existing element. In this context, the admissible error definition is directly dependent on the definition of number of elements. According to the convergence rates of the recovered gradient of the solution, the convergence rate of the errors is given by Eq. (10). The error in energy norm for a linear approximation can be defined in the current mesh and next mesh expressed with subscript *old* and *new*, respectively, as

$$\|e_{old}\|^{2}=\int_{\Omega_{ie}}U_{old}\,d\Omega\le C^{2}h_{old}^{2}, \tag{29}$$

and

$$\|e_{new}\|^2 = \int_{\Omega_{ie}} U_{new}\, d\Omega \le C^2 h_{new}^2. \tag{30}$$

Relating Eq. (29) and Eq. (30), and considering that the domain and constant C remains the same, the average value of the error density function in energy can be expressed as:

$$\bar{U}_{old}\,|\Omega_o| \le \left(C h_{old}^{\alpha}\right)^2, \tag{31}$$

$$\bar{U}_{new}\,|\Omega_o| \le \left(C h_{new}^{\alpha}\right)^2, \tag{32}$$

and

$$\bar{U}_{new} = \mu \bar{U}_{old}, \text{ with } \mu = \left(h_{new} / h_{old}\right)^2. \tag{33}$$

Applying this concept to the quadratic equation of the error density function in energy, Eq. (16) can be expressed as

$$U_{new} = \mu\left(U_0 + \boldsymbol{Gx} + \boldsymbol{x}^T \boldsymbol{Hx}\right) \tag{34}$$

Thus, an iterative process can be described redefining the error density function in energy taking in consideration the predicted element size and number of elements in the new mesh as:

Step 1: Estimate the element parameters, i.e., U_0, $tr(\boldsymbol{H})$, according to Eq. (16) , ε_{adm}^2 according to Eq. (9) and the new element sizes according to Eq. (28).

Step 2: For each element, the parameter μ is evaluated considering the estimated size of the element in the next mesh and current mesh. The element parameters are then updated as well as the element sizes.

Step 3: Estimate the number of elements in the next mesh (NEL_{new}) and update the admissible error, ε_{adm}^2. These parameters are evaluated using the following equations

$$NEL_{new} = \sum_{ie=1}^{NEl} \left(h_{new} / h_{old}\right)^2 \text{ and } \varepsilon_{adm} = \bar{\eta}\,\|u\| \Big/ \sqrt{NEl}\,.$$

Step 4: Check convergence.

4 ISOTROPIC ERROR DENSITY NODAL RECOVERY (IEDNR) MESH DESIGN

As mentioned, the main contribution of this paper is to introduce and analyze a modification to the IEDR mesh design technique for h-adaptive FEM processes. The proposed methodology, here named IEDNR, takes in consideration the limitations imbued to the IEDR technique and aims at improving them. Initially, it is observed the necessity for mesh design methodologies to be functional for different orders of element approximation.

Thus, the IEDNR methodology is put forward as a basis for the generalization of the technique for higher order finite elements. Further, the original methodology requires post processing of the element sizes in the evaluation of the nodal parameters required by common mesh generators. Specifically, the BAMG mesh generator, based on nodal parameters, is used in the analysis of both IEDR and IEDNR techniques. The post-process of element size is avoided by evaluating a new nodal error density function in energy for each node of the mesh. A nodal iterative admissible error evaluation process is also introduced based on the minimum required number of elements in the next mesh.

4.1 Nodal recovered error density function in energy and element design

In this section, the IEDNR technique is described for a generic problem, considering linear triangular finite elements. A quadratic error density function in energy norm for each element is evaluated similarly to the original technique, Eq. (14), obtained through a polynomial approximation

$$U_{approx}(x,y) = a_{U_1} + a_{U_2}x + a_{U_3}y + a_{U_4}x^2 + a_{U_5}xy + a_{U_6}x^2 = \boldsymbol{P}_q^{\,T}\boldsymbol{a}_U \,, \tag{35}$$

where U_{approx} is the approximated quadratic error density function in energy norm obtainable for higher order elements through the use of polynomial approximation, a_{U_1} to a_{U_6}, are the coefficients of the polynomial function which forms $\boldsymbol{a}_U$, $\boldsymbol{P}_q$ is a vector containing the relative coordinates of the quadratic polynomial in relation to the barycenter of the element. In the literature, several polynomial approximation techniques are available (Borwein and Erdélyi, 1995). The function can be re-arranged and expressed similarly to the IEDR technique, thus

$$U_{approx}(x,y) = U_{0_{ie}} + \left(G_{1_{ie}}x + G_{2_{ie}}y\right) + \left(H_{11_{ie}}x^2 + 2H_{12_{ie}}xy + H_{22_{ie}}y^2\right) \tag{36}$$

A patch of elements composed by all the elements connected to the *j-th* node is formed. The quadratic error density function of each element is evaluated. The origin of an element's error density function in energy is located in that element's barycenter.

4.1.1 Shifting the error distribution to the vicinity of the node

In order to express a single error density function in energy describing the central node of the patch, it is required to scale the patch and its functions to the vicinity of the central node. This is performed by creating a virtual element and decreasing the size of the patch according to this element's area. Figure 1 illustrates this procedure.

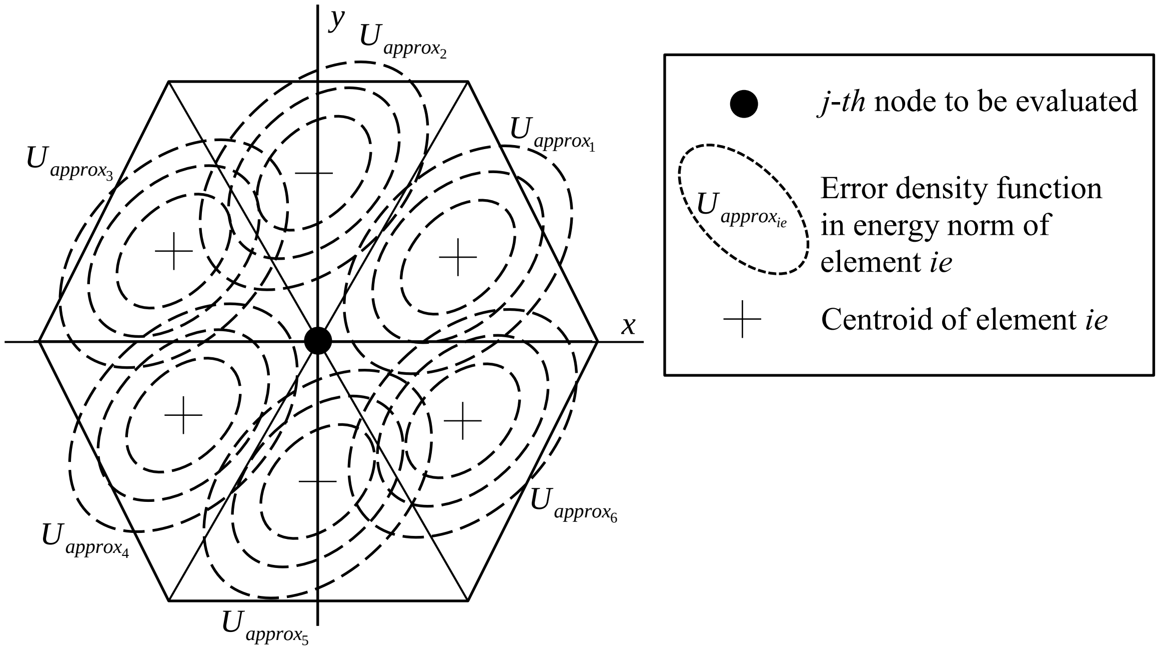

Figure 1: Illustration of patch of elements and their approximated quadratic error density functions in energy norm.

A virtual element is created centered at the node to be evaluated. The concept behind this methodology is to scale the distribution of errors of the patch connected to a node using a virtual element size. After that, the optimal element size is calculated by adjusting the coordinates of each element's barycenter (origin of the error density function). Figure 2 illustrates the miniaturized patch and the relative coordinates of an element's barycenter.

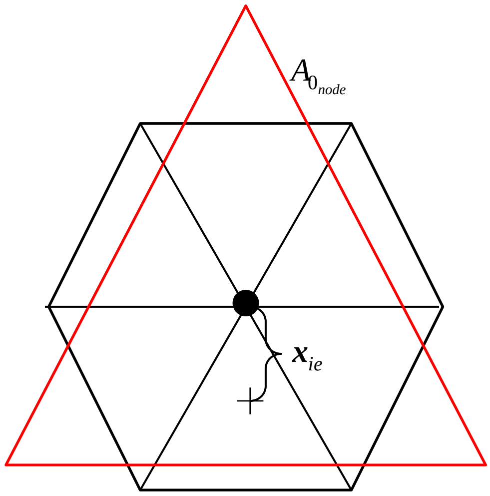

Figure 2: New patch domain scaled according to the average of the original elements areas

Thus, the area of the virtual element, $A_{0_{node}}$, is given by the average of the patch element's areas, $A_{0_{ie}}$, expressed as

$$A_{0_{node}} = \frac{1}{NEP}\sum_{ie=1}^{NEP} A_{0_{ie}} \,, \tag{37}$$

where NEP denotes the number of elements in the patch. The virtual element's error density function in energy, U_j, is calculated by adding each element's error density functions, positioned at their respective adjusted origins, and dividing them by the number of elements. The equation can be expressed as

$$U_j(x,y) = \left[\frac{1}{NEP}\sum_{ie=1}^{NEP}\left(U_{0_{ie}} + \left(G_{1_{ie}} x_{ie} + G_{2_{ie}} y_{ie}\right) + \left(H_{11_{ie}} x_{ie}{}^{2} + 2H_{12_{ie}} x_{ie} y_{ie} + H_{22_{ie}} y_{ie}{}^{2}\right)\right)\right], \tag{38}$$

where x_{ie} and y_{ie} compose the coordinate system of each element's function. In order to shift this origin, a relation between each scaled element's barycenter coordinates is defined as

$$\boldsymbol{x}_{ie} = \begin{bmatrix} x - x_{0_{ie}} \\ y - y_{0_{ie}} \end{bmatrix}, \tag{39}$$

where $x_{0_{ie}}$ and $y_{0_{ie}}$ denotes the relative coordinates between the adjusted origin of each element's error density function in energy and the nodal coordinates, x_{node} and y_{node}. Initially, these relative coordinates can be described considering equilateral triangles and Eq. (37), thus

$$x_{0_{ie}} = \left(\frac{x_{Bar_{ie}} - x_{node}}{\sqrt{NEP}}\right), \tag{40}$$

$$y_{0_{ie}} = \left(\frac{y_{Bar_{ie}} - y_{node}}{\sqrt{NEP}}\right), \tag{41}$$

where $x_{Bar_{ie}}$ and $y_{Bar_{ie}}$ denotes the coordinates of the barycenter of element *ie* located on the patch.

4.1.2 Adjustment of function transformation according to element error

Having determined an initial shift in each element's error density functions, an additional adjustment is required to make sure that the shifted distribution accurately describes the original error density function of each element, such that an overestimate or underestimate of error does not occur. The integral of the shifted element's error density function over the virtual triangular domain, E_{Shift}, is required to be equal to the integral of the unshifted function over the original element, E_{ie}. Figure 3 describes this process. This adjustment is based on the convergence of the solution as described by Eq. (10), thus

$$\frac{\|E_{ie}\|}{\|E_{Shift}\|} \propto \frac{Ch_{0_{ie}}^{p}}{Ch_{ie}^{p}} \propto \frac{\boldsymbol{x}}{\boldsymbol{x}_{0_{ie}}} \,, \tag{42}$$

$$\boldsymbol{x} = \boldsymbol{x}_{0_{ie}} \frac{h_{0_{ie}}^{p}}{h_{ie}^{p}} \text{ such that } \|E_{ie}\| = \|E_{Shift}\|, \tag{43}$$

Proceedings of the XXXVIII Iberian Latin-American Congress on Computational Methods in Engineering
P.O. Faria, R.H. Lopez, L.F.F. Miguel, W.J.S. Gomes, M. Noronha (Editores), ABMEC, Florianópolis, SC, Brazil, November 5-8, 2017.

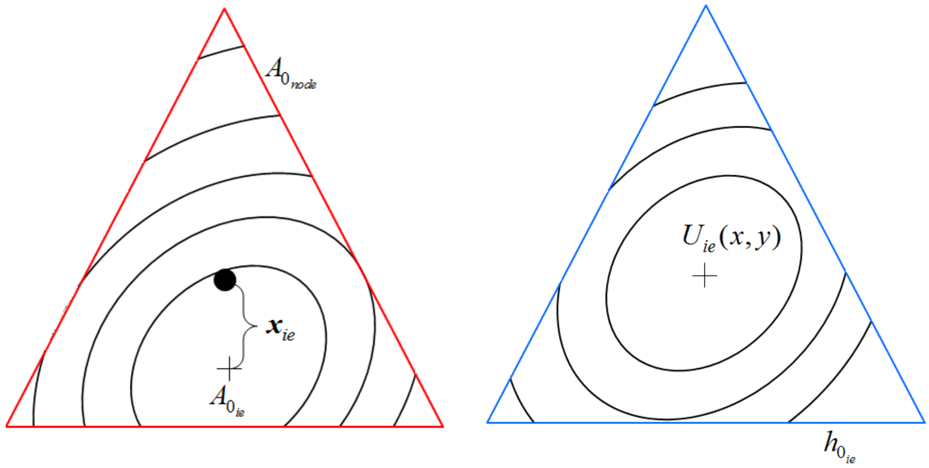

Figure 3: In red, the error density function of an element is transformed (its origin is moved proportionally to the element size) to equate the error contained for that original element (in blue).

where the error of the element *ie*, E_{ie}, is calculated utilizing Eq. (24) and its original size, $h_{0_{ie}}$., thus

$$E_{ie}^2 = h_{0_{ie}}{}^2\left[\alpha U_{0_{ie}} + \beta tr\left(\boldsymbol{H}_{ie}\right) h_{0_{ie}}{}^2\right], \tag{44}$$

Then, a new size of element, h_{ie}, is calculated using the shifted error density function in relation to the central node of the patch, such that it contains the error of the original element (E_{ie}). This is evaluated via Eq. (28) by substituting the admissible error for the element error:

$$h_{ie} = \left(\frac{\sqrt{\left(\alpha U_{Shift_{ie}}\right)^2 + 4\beta tr\left(\boldsymbol{H}_{ie}\right) E_{0_{ie}}^2} - \alpha U_{shift_{ie}}}{2\beta tr\left(\boldsymbol{H}_{ie}\right)}\right)^{1/2}, \tag{45}$$

where $U_{Shift_{ie}}$ denotes the constant term of the shifted function, given by

$$U_{Shift_{ie}} = U_{0_{ie}} - G_{1_{ie}} x_{0_{ie}} - G_{2_{ie}} y_{0_{ie}} + H_{11} x_{0_{ie}}{}^2 + H_{22} y_{0_{ie}}{}^2 + 2H_{12} x_{0_{ie}} y_{0_{ie}}. \tag{46}$$

Considering the initial scaling of the patch and the additional adjustment described above (Eq. (43)), the relative coordinates between the adjusted origin of the error density functions and the central node coordinates, $x_{0_{ie}}$ and $y_{0_{ie}}$, is given as

$$x_{0_{ie}} = \left(\frac{x_{Bar_{ie}} - x_{node}}{\sqrt{NEP}}\right)\frac{h_{0_{ie}}}{h_{ie}}, \tag{47}$$

$$y_{0_{ie}} = \left(\frac{y_{Bar_{ie}} - y_{node}}{\sqrt{NEP}}\right)\frac{h_{0_{ie}}}{h_{ie}}. \tag{48}$$

4.1.3 New element size design via optimization

The optimal element sizes are calculated using an error density function for each node. These functions are expressed as the average of the shifted error density functions for each element contained in the nodal patch. Thus, rearranging Eq. (21), the error contained in the triangular region, Ω_{node}, can be described as

$$\begin{aligned}
\|e\|^2_{\Omega_{node}} &= E^2_{node} = \int_{\Omega_{node}} U_j(x,y)\, d\Omega \\
&= \int_{\Omega_{node}} \frac{1}{NEP} \sum_{ie=1}^{NEP} U_{0_{ie}} + \left(G_{1_{ie}} x_{ie} + G_{2_{ie}} y_{ie}\right) + \left(H_{11_{ie}} x_{ie}{}^2 + 2H_{12_{ie}} x_{ie} y_{ie} + H_{22_{ie}} y_{ie}{}^2\right) d\Omega \\
&= \frac{1}{NEP} \sum_{ie=1}^{NEP} \left[U_{0_{ie}} - G_{1_{ie}} x_{0_{ie}} - G_{2_{ie}} y_{0_{ie}} + H_{11_{ie}} x_{0_{ie}}{}^2 + H_{22_{ie}} y_{0_{ie}}{}^2 + 2H_{12_{ie}} x_{0_{ie}} y_{0_{ie}}\right] \int_{\Omega_{node}} d\Omega \\
&+ \frac{1}{NEP} \sum_{ie=1}^{NEP} H_{11_{ie}} \int_{\Omega_{node}} x^2\, d\Omega + \frac{1}{NEP} \sum_{ie=1}^{NEP} H_{22_{ie}} \int_{\Omega_{node}} y^2 d\Omega \\
&= U_{0_j} A_{0_{node}} + H_{11_j} I_{y_{node}} + H_{22_j} I_{x_{node}},
\end{aligned} \tag{49}$$

$A_{0_{node}}$, $I_{y_{node}}$ and $I_{x_{node}}$ are calculated via Eq. (23) and the new terms are redefined as

$$U_{0_j} = \frac{1}{NEP} \sum_{ie=1}^{NEP} \left[U_{0_{ie}} - G_{1_{ie}} x_{0_{ie}} - G_{2_{ie}} y_{0_{ie}} + H_{11} x_{0_{ie}}{}^2 + H_{22} y_{0_{ie}}{}^2 + 2H_{12} x_{0_{ie}} y_{0_{ie}}\right], \tag{50}$$

$$H_{11_j} = \frac{1}{NEP} \sum_{ie=1}^{NEP} H_{11_{ie}}, \tag{51}$$

$$H_{22_j} = \frac{1}{NEP} \sum_{ie=1}^{NEP} H_{22_{ie}}. \tag{52}$$

The size of the new element is then calculated similarly to the IEDR methodology by using the optimization problem stated in Eq. (25). The new element size estimated for the node *j* is estimated as

$$h_{new} = \left(\frac{\sqrt{\left(\alpha U_{0_j}\right)^2 + 4\beta tr\left(\boldsymbol{H}_j\right)\varepsilon^2_{adm}} - \alpha U_{0_j}}{2\beta tr\left(\boldsymbol{H}_j\right)} \right)^{1/2}. \tag{53}$$

4.1.4 Admissible error update considering optimal mesh (nodal)

Similarly to the IEDR technique, an iterative process is utilized to update the admissible error and error density function's parameters considering the expected number of elements in the new mesh. Here a modification is also introduced due to the nodal evaluation of the error function. The steps are shown below:

Step 1: Estimate the nodal parameters, i.e., U_{0_j}, $tr\left(\boldsymbol{H}_j\right)$, according to Eq. (47), Eq. (48) and Eq. (49) , the ε^2_{adm} according to Eq. (8), and the new element sizes according to Eq. (50).

Proceedings of the XXXVIII Iberian Latin-American Congress on Computational Methods in Engineering
P.O. Faria, R.H. Lopez, L.F.F. Miguel, W.J.S. Gomes, M. Noronha (Editores), ABMEC, Florianópolis, SC, Brazil, November 5-8, 2017.

Step 2: For each node, a parameter β is evaluated considering the estimated size of the element in the next mesh and current mesh. The node parameters are then updated as well as the element sizes.

Step 3: Estimate the number of elements in the next mesh (NEL_{new}) and update the admissible error ε_{adm}^2 . Relating the number of nodes in the mesh, $Notot$, and using an average of the elements sizes to find h_{old} for the first iteration, these parameters are evaluated continuously:

$$NEL_{new} = \frac{NEl}{Notot}\sum_{N=1}^{Notot}\left(h_{new}/h_{old}\right)^2 \text{ and } \varepsilon_{adm} = \bar{\eta}\left\|u\right\|/\sqrt{NEl}\,.$$

Step 4: Check convergence

5 RESULTS

In order to illustrate the quality of the IEDNR adaptive design, two scalar linear problems are tackled utilizing the SPR error estimation and CST elements are considered. The results are compared to the Ch^p, IEDR and IEDNR mesh designs. The implementation was done in Matlab and the mesh was generated through BAMG (Hecht, 2012).

5.1 Problem 1

Considering a problem defined by Eq. (1), the domain excitation is applied such that the analytic solution is given by (modified from Mitchel, 2013)

$$T(x,y) = 2^{2(a+b)}x^a(1-x)^a y^b(1-y)^b, \tag{54}$$

where $a = 20$ and $b = 1$. The h-adaptive processes are compared based on the Ch^p, IEDR and IEDNR mesh designs. For all three processes, the gradient recovery is generated via the SPR technique and linear triangular finite elements are used. The initial mesh is composed of 244 uniform elements and the admissible global error is $\bar{\eta} = 5\%$. Figure 4 demonstrates the error distribution and initial mesh for the design techniques.

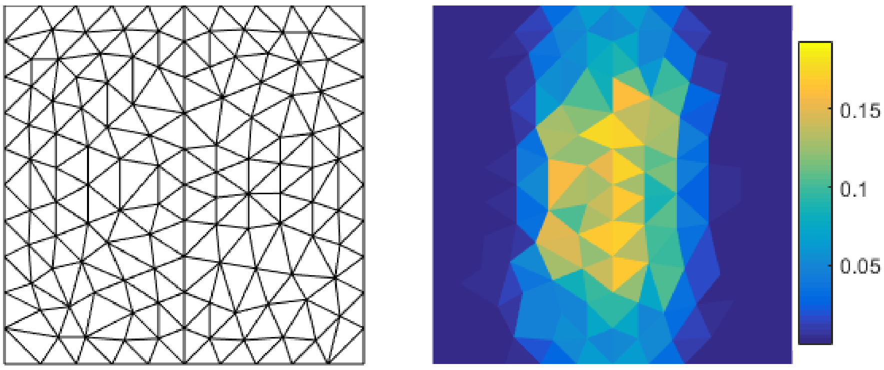

(a) (b)

Figure 4: Problem 1: (a) initial mesh and (b) error distribution.

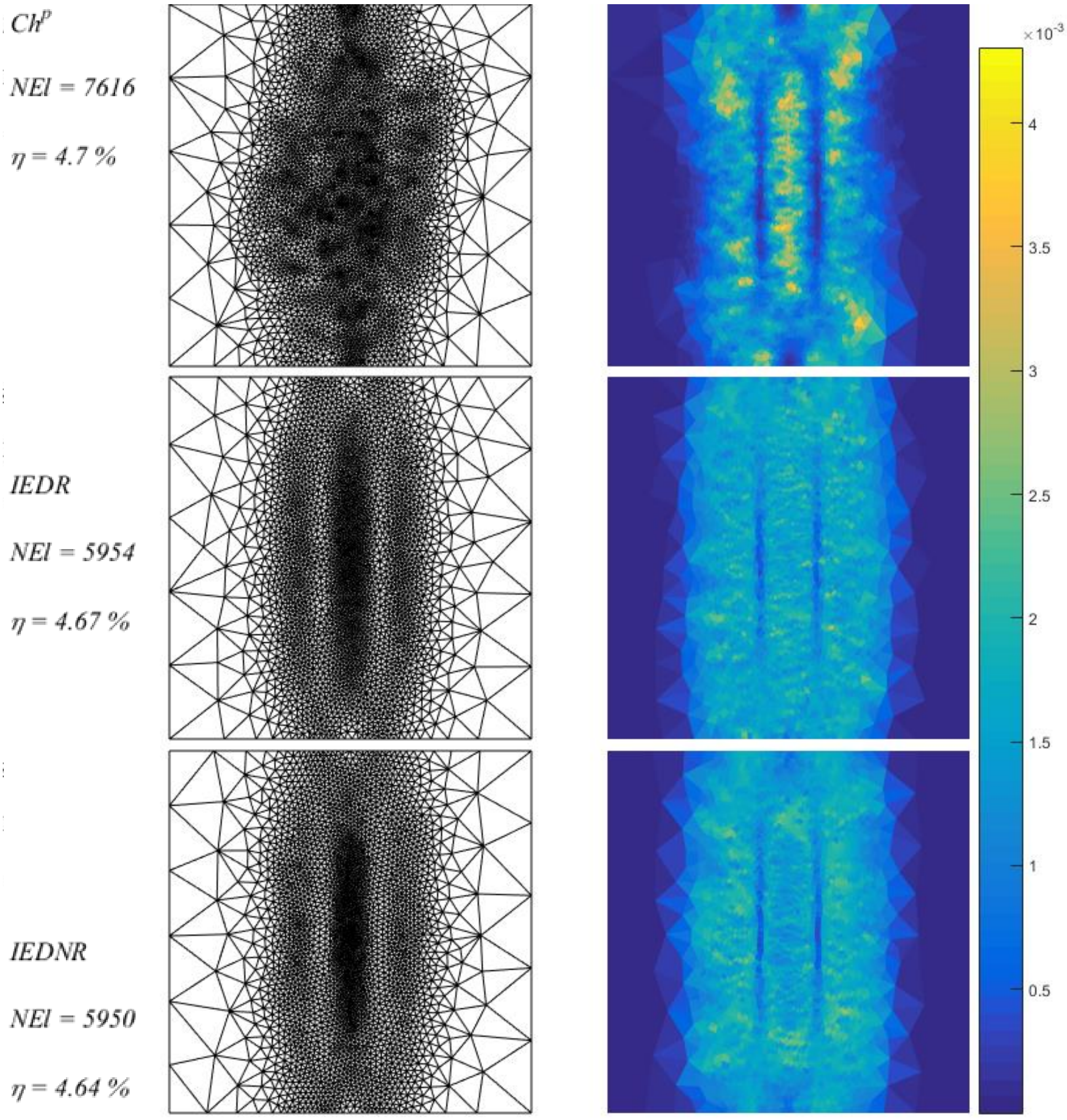

Figure 5: Problem 1: (a) Final mesh refinement iteration (*it*=3) comparing *Ch^p*, IEDR and IEDNR techniques and (b) their analytical error distributions.

In Fig. 5, a comparison between the final meshes (*iteration* = 3) for each refinement technique analyzed is shown, where η denotes the estimated error. It is perceptible that the IEDR and IEDNR techniques reached a similar final mesh. The number of elements of both IEDR and IEDNR are approximately 23% lower than those of the Ch^p refinement strategy showing efficient refinement. Also, the IEDNR technique tends to refine the mesh slight more in regions with higher error and slight less in the other regions when compared to the IEDR methodology. This effect counteracts one another producing a similar total analytical error while producing a slightly different mesh when compared to the IEDR technique. Figure 6 demonstrates the convergence of the techniques and the deviation of the element local error parameter. The parameter ($D_{\bar{\zeta}}$) gives an indicative whether the error is well distributed in the mesh, expressed by the following equation (Pereira et al., 2016)

$$D_{\bar{\zeta}} = \sqrt{\frac{\sum_{ie=1}^{NEl}\left(\zeta_{ie}-1\right)^2}{NEl}}. \tag{55}$$

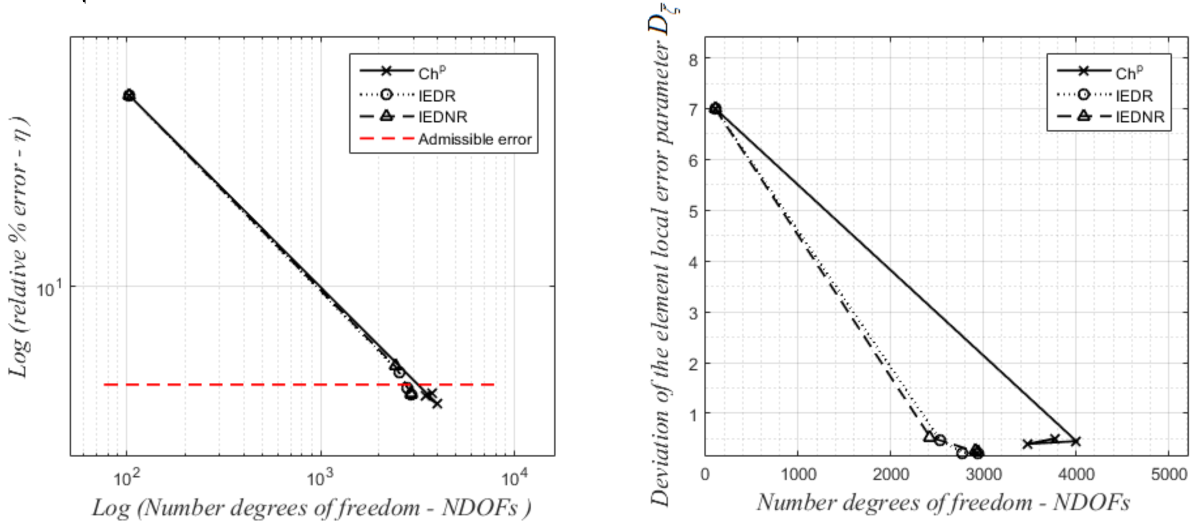

(a) (b)

Figure 6: Problem 1: (a) Convergence of the tecniques demonstrated by Log (Number of degrees of freedom) x Log (relative % error). (b) Deviation of the element local error parameter for each iteration.

The distribution parameter indicates that both IEDR and IEDNR distribute the error similarly, showing better results when compared to the *Ch*^{p} technique. From the results, the IEDNR technique demonstrates stability when compared to other techniques, having a change in the number of elements from 5890 to 5950 (1.01%) between iterations 2 and 3 (5.92% for IEDR and 8.46% for the *Ch*^{p} technique).

5.2 Problem 2

In this example, the domain excitation gives an analytical solution as (Zienkiewicz and Taylor, 2000)

$$u(x, y) = x(1-x)y(1-y)\arctan\left[\alpha(\rho-\rho_0)\right], \tag{56}$$

where $\rho=(x+y)/\sqrt{2}$, $\rho_0=0.8$ and $\alpha=20$. The same admissible global error is provided as the last problem ($\bar{\eta}=5\%$) and the initial mesh contains 244 elements. Figure 7 demonstrates the finite element meshes for the h-adaptive IEDNR mesh refinement process. This image demonstrates that the IEDNR mesh refinement technique is smooth, with little oscillation between meshes, occurrence found when utilizing the *Ch*^{p} technique. Similarly to problem 1, Fig. 8 and Fig. 9 illustrate that the IEDNR and IEDRN techniques exhibit, in general, better mesh parameters than the *Ch*^{p} projection.

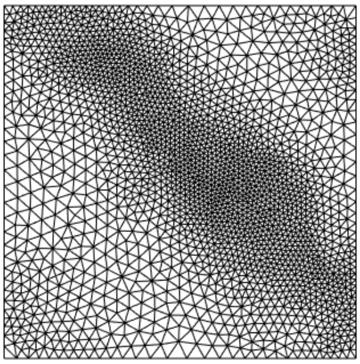

(a)

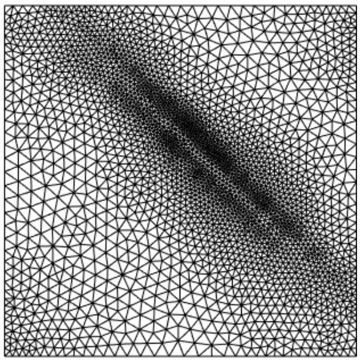

(b)

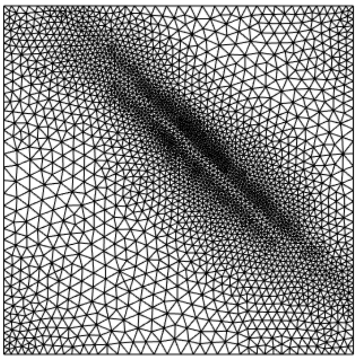

(c)

Figure 7: Problem 2: Finite element meshes for IEDNR mesh design: (a) Iteration 1, *NEl* = 4507, $\eta = 5.74\%$. (b) Iteration 2, *NEl* = 5582, $\eta = 4.81\%$. (c) Iteration 3, *NEl* = 5641, $\eta = 4.71\%$.

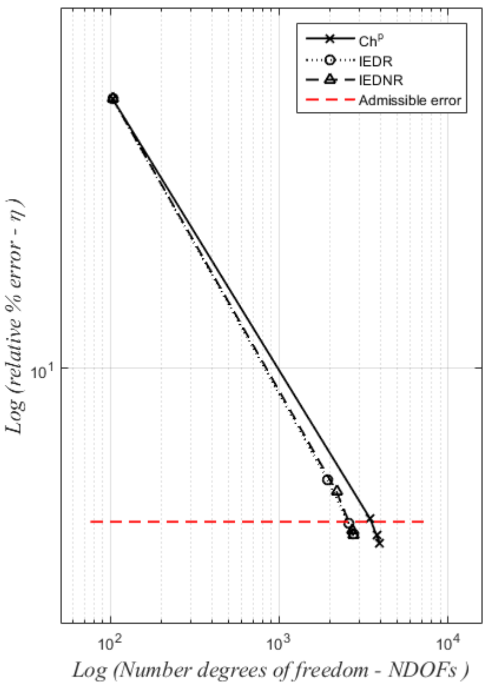

(a)

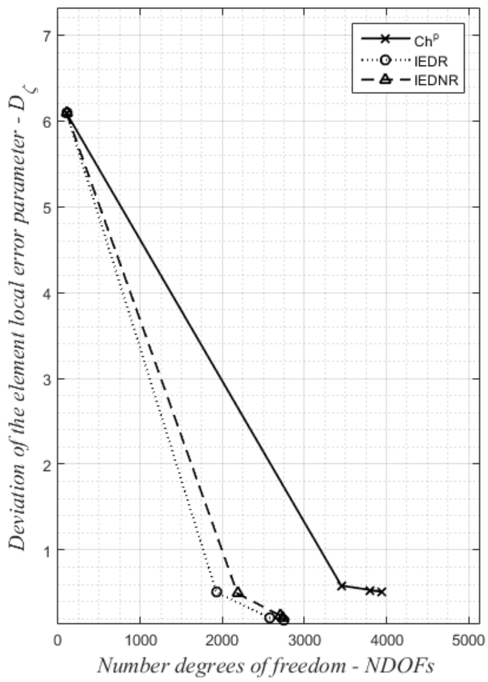

(b)

Figure 8: Problem 2: (a) Convergence of the tecniques demonstrated by Log (Number of degrees of freedom) x Log (relative % error). (b) Deviation of the element local error parameter for each iteration

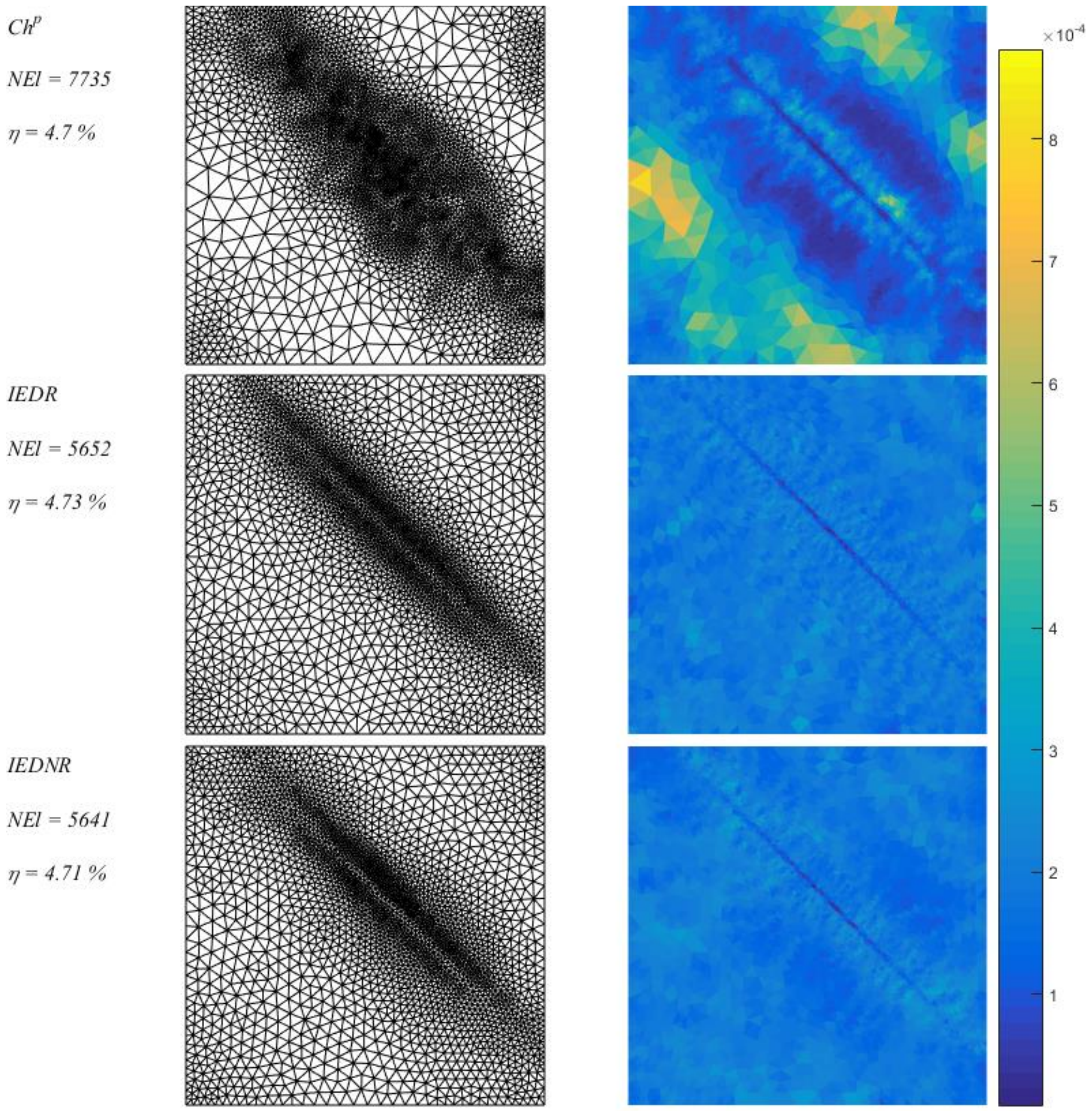

(a) **(b)**

Figure 9: Problem 2: (a) Final mesh refinement iteration (*it*=3) comparing *Ch*^{p}, IEDR and IEDNR techniques and (b) their analytical error distributions.

Observing Fig. 7, Fig. 8 and Fig. 9, it can be seen that better mesh parameters for the IEDR and IEDNR techniques are obtained when compared to the results found using the *Ch*^{p} methodology. In this problem, an abrupt change in the solution is present in the diagonal direction. The IEDNR technique is able to characterize this abrupt change employing a sharp contrast of element sizes in the region as seen in Fig. 9. Further, the mesh parameters of Fig 8 show a linear approach to the desired solution.

6 CONCLUSION

The current paper proposes a modification to the IEDR technique taking in consideration a nodal recovery of the error density function in energy. Named IEDNR, the technique was implemented and analyzed for linear scalar problems. The results show that the modification is equally precise as the IEDR technique, while presenting better mesh parameters when compared to the mesh design proposed by Zienkiewicz and Zhu, here referred to as Ch^p design. Furthermore, the proposed modification is introduced as a basis for the generalization of the IEDR technique for higher order elements.

ACKNOWLEDGEMENTS

The authors would like to thank the *Programa de Pós-Graduação em Engenharia Mecânic*a at *Universidade Federal do Paraná* and the *Universidade Tecnológica do Paraná* for the support in completing this study.

REFERENCES

Ainsworth, M., & Oden, J. T., 2000. *A Posteriori Error Estimation in Finite Element Analysis*, 1. ed., John Wiley and Sons.

Boroomand, B., & Zienkiewicz, O. C., 1997. Recovery by equilibrium in patches. *International Journal for Numerical Methods in Engineering*, vol. 40, pp. 137–164.

Borwein, P. & Erdélyi, T., 1995. *Polynomials and Polynomials Inequalities, Graduate Texts in Mathematics*, 1. ed., Springer-Verlag.

Castellazzi, G., Miranda, S., & Ubertini, F., 2010. Adaptivity based on the recovery by compatibility in patches. *Finite Elements in Analysis and Design*, vol. 46, pp. 379–390.

Cook, R. D., Malkus, D. S., Plesha, M. E., & Witt, R. J., 2002. *Concepts and applications of finite element analysis*, John Wiley and Sons.

Silva, J. & Pereira, J. T., 2017. h-adaptive topology optimization based on rapid oscillation of material properties. *Latin American Journal of Solids and Structures.* Submitted.

Díez, P., & Huerta, A., 1999. A unified approach to remeshing strategies for finite element h-adapativity. *Computer Methods in Applied Mechanics and Engineering*, vol. 176, pp.215-229

Hecht, F., 2012. New development in FreeFem++. Journal of Numerical Mathematics, vol. 20, pp. 251-265.

Huang, Y., & Yi, N., 2010. The Superconvergent Cluster Recovery Method. *Journal of Scientific Computing*, vol. 44, pp. 301–322.

Li, L., & Bettess, P., 1995. Notes on mesh optimal criteria in adaptive finite element computations. *Communications in Numerical Methods in Engineering*, vol. 11, pp.911-915

Mitchell, W. F., 2013. A collection of 2D elliptic problems for testing adaptive grid refinement algorithms. *Applied Mathematics and Computation*, vol. 220, pp. 350-364

Oden, J.T., & Reddy, J.N., 2011. *An Introduction to the Mathematical Theory of Finite Elements*, 2. ed., Dover Publications (Chapter 8).

Onãte, E., & Bugeda, G., 1993. A study of mesh optimality criteria in adaptive finite element analysis. *Engineering Computations*, vol. 10, pp. 307–321

Pereira, J. T., Silva, J., & Gonçalves, J. C. L., 2016. Método dos elementos finitos h-adaptativo: uma nova técnica para projeção isotrópica do tamanho elementar. *Proceedings of the XXXVII Iberian Latin-American Congresso on Computational Methods in Engineering.*

Reddy, J. N., 2006. *An Introduction to the Finite Element Method*. 3. ed., Mc Graw Hill

Ubertini, F., 2004. Patch recovery based on complementary energy. *International Journal for Numerical Methods in Engineering*, vol. 59, pp. 1501–1538

Wiberg, N. E., & Abdulwahab, F., 1992. An efficient postprocessing technique for stress problems based on superconvergent derivatives and equilibrium. *Numerical Methods in Engineering*, pp. 25–32.

Wiberg, N. E., Abdulwahab, F., & Li, X. D., 1997. Error estimation and adaptive procedures based on Superconvergent Patch Recovery (SPR) techniques. *Archives of Computational Methods in Engineering*, vol. 4, pp. 203–242.

Wiberg, N. E., Abdulwahab, F., & Ziukas, S., 1994. Enhanced superconvergent patch recovery incorporating equilibrium and boundary conditions. *International Journal for Numerical Methods in Engineering*, vol. 37, pp. 3417–3440.

Zhang, Z., & Naga, A., 2005. A new finite element gradient recovery method: Superconvergence Property. *SIAM Journal on Numerical Analysis*, vol. 26, pp. 1192–1213.

Zienkiewicz, O. C., & Zhu, J. Z., 1987. A simple error estimator and adaptive procedure for practical engineering analysis. *International Journal for Numerical Methods in Engineering*, vol. 24, pp. 337–357.

Zienkiewicz, O. C., & Zhu, J. Z., 1992a. The superconvergent patch recovery and a posteriori error estimates. Part 1: the recovery technique. *International Journal for Numerical Methods in Engineering*, vol. 33, pp. 1331–1364.

Zienkiewicz, O. C., & Zhu, J. Z., 1992b. The superconvergent patch recovery and a posteriori error estimates. Part 2: Error estimates and adaptivity. *International Journal for Numerical Methods in Engineering*, vol. 33, pp.1365–1382.

Zienkiewicz, O. C., Taylor, R. L., 2000. *The Finite Element Method*. *Volume 1: The Basis.* Butterworth Heinemann.